Denoising of Impulse Noise using Partition-Supported Median, Interpolation and DWT in Dental X-Ray Images

Mohamed Shajahan[1], Siti Armiza Mohd Aris[2], Sahnius Usman[3], Norliza Mohd Noor[4]
Razak Faculty of Technology and Informatics, Universiti Teknologi Malaysia
Kuala Lumpur Campus, Jalan Sultan Yahya Petra, Malaysia[1, 2, 3, 4]
University of Business and Technology, Jeddah, Saudi Arabia[1]

***Abstract*—The impulse noise often damages the human dental X-Ray images, leading to improper dental diagnosis. Hence, impulse noise removal in dental images is essential for a better subjective evaluation of human teeth. The existing denoising methods suffer from less restoration performance and less capacity to handle massive noise levels. This method suggests a novel denoising scheme called "Noise removal using Partition supported Median, Interpolation, and Discrete Wavelet Transform (NRPMID)" to address these issues. To effectively reduce the salt and pepper noise up to a range of 98.3 percent noise corruption, this method is applied over the surface of dental X-ray images based on techniques like mean filter, median filter, Bi-linear interpolation, Bi-Cubic interpolation, Lanczos interpolation, and Discrete Wavelet Transform (DWT). In terms of PSNR, IEF, and other metrics, the proposed noise removal algorithm greatly enhances the quality of dental X-ray images.**

***Keywords*—Salt and pepper noise; impulse noise; X-ray noise removal; X-ray teeth image quality enhancement; dental X-ray noise reduction**

I. Introduction

X-ray, CT, and MRI-like medical devices generate many medical images to help doctors. The impulse noise contaminates the medical image pixels, damaging the real data [1]. Currently, X-Ray images are the primary sources for diagnosing dental diseases [2]. The dental diagnosis via dental-X-ray images is a trustful field that provides the exact outcome in dentistry, and it faces the real test of the contingency of impulse noise. The impulse noise is also known as salt and pepper noise. As stated in [3], identifying Dental-images in X-ray is crucial for any intuitive assessment of the denoising of impulse. Impulse noise causes a complete loss of image information, which lowers the quality of X-RAY images [4] [5]. Therefore, impulse noise in dental X-ray images must be addressed. An essential step in any process of enhancing and diagnosing Dental-X-ray images is noise removal [6]. Transmission, acquisition, image processing, and storage are the main causes of impulsive noise. The salt noise has an intensity of 255, whereas the pepper noise has a value of zero [7] [8]. Hence, impulse noise reduction is a crucial part of human dental X-Ray image diagnosis.

A noise removal approach that fixes the corrupted images using either the median or the adjacent pixel value was proposed by Srinivasan et al. [14]. The problem is that they are unsuitable for low-range noises. Pitas et al. [10] presented a Nonlinear mean filter that works based on the nonlinear-means concept to eliminate impulse noises. The short range of noise reduction is the flaw. Zhang and Li [22] describe an adaptive weighted mean filter (AWMF) to remove impulse noise, especially in images containing high-level noises. The limitation is that the computational time of the work increases in high noise-contaminated images. To sharpen or enlarge the digital image bicubic interpolation is used [31].

Tracey et al. [17] described an enhanced non-local means (NLM) based noise removal technique for X-ray scatter (XBS) images. The edges are not appropriately preserved in this work which is a drawback of this model. Kundu [18] proposes a noise removal method using the PND-NLM technique in X-ray images. The method employs enhancement of X-ray images of bones using Gaussian higher-order derivative operation. X-ray teeth images are not considered in this model, which is a limitation of this work. Shi et al. [16] describe a noise removal technique in real-time X-ray images as it encounters high noise and low contrast. After computing the relationship between noise variance and grayscale value, a modified adaptive noise reduction filter is used to filter the image. Some optimization in work is essential to address the low contrast issue. Shanida et al. [19] suggest a wavelet-based noise removal and enhancement method to address the high noise and low contrast issue in X-Ray teeth images. This work cannot process huge-noise-density teeth X-ray images. Naouel et al. [23] suggest a noise removal and localization method using discrete wavelet transform and thresholding methods. This model extracts seven Regions of Interest from the images, which consumes more time which is a drawback of this work.

Khan et al. [20] developed a Poisson noise and impulse noise removal method based on an improved layer discrimination approach in X-Ray images. The edges are not preserved correctly in this model which is a disadvantage of this work. Markarian et al. [21] propose a denoising method in a compressive sensing framework using high–order total variation method in SAR images. It adopts method based on MAP estimation for denoising and recovering large-size complex SAR images. The thickness of objects in images becomes bulky unnaturally. A noise suppression technique for X-ray images was created by Mandic et al. [24] by altering the intersection of confidence intervals. The relative Intersection of the Confidence Intervals rule is the name of this set of rules.

The teeth X-ray has not been used to examine this work. The existing noise reduction methods suffer from mitigated Peak signal-to-noise ratio, blurred edges, and incapable to resolve a massive range of noises. The proposed NRPMID filter resolves the above issues. It reduces the impulse noise in dental X-ray images. The NRPMID filter is constructed using partition-based Median filter, Interpolation, and DWT techniques. To achieve high denoising accuracy, a new rule set is developed. The partition-based methods are employed according to this new rule set. The biggest drawback that they experience is the noise that is added as a result of the wave's transmitted coherent nature. The image is distorted by these sounds, which might also lead to misidentification. There is a variety of noise in every one of those medical imaging systems. The x-ray images, for instance, are frequently distorted by Poisson noise, salt and pepper noise, and speckle noise. Before continuing with subsequent image processing operations, it is imperative to remove salt-and-pepper noise since this type of noise greatly contaminates images and does severe harm to any knowledge or data that may have been contained in the original image. To overcome certain drawbacks the proposed method is used. The primary contributions of this work are the partition-based methodology and the efficient rule construction.

Section I includes the introduction section. Section II explains the literature review. Section III explains the proposed work, section IV assesses the performance of the NRPMID filter. Section V notifies the conclusion statements about the NRPMID method.

II. Literature Review

Hawang et al. [9] focused on two algorithms, namely Ranked-order based Adaptive Median Filter (RAMF) and Size based Adaptive Median Filter (SAMF), for denoising the impulse noise. Herein, multiple-size window kernels are used. The surrounding noisy pixels badly impact the denoising quality.

Tao et al. [11] introduced an image enhancement technique to denoise impulse noise based on Tri-state Median Filter (TSMF). Herein, two concepts are used: Standard Median (SM) filter and the Centre Weighted Median (CWM) filter.

Chen and Lien [13] proposed a novel algorithm for removing impulse noise from corrupted images. It employs an efficient impulse noise detector to detect the noisy pixels and an edge-preserving filter to reconstruct the intensity values of noisy pixels.

Gouchol et al. [12] designed a denoising algorithm for impulse noise by performing the Selective removal of impulse noise. This approach works based on homogeneity level information of an image. This work has used the fixed window kernels, which is the disqualification.

Toh et al. [15] described a two-stage noise adaptive technique for eliminating salt-and-pepper noise. The method is based on a fuzzy switching median filter for noise detection and removal. Herein, noisy pixels are determined based on the histogram concept. The artifact generated by the filtering process is found using fuzzy reasoning. The drawback is substantial cost consumption, which has negative effects when used in complicated systems.

III. Methodology

The proposed denoising method NRPMID removes impulse noise from Dental X-RAY images using the eight concepts such as Mean filter, Median filter, Bi-linear interpolation-based filter, Partition based Median filter, Bi-cubic interpolation-based filter, Partition based Bi-cubic interpolation-based filter, Partition based Lanczos interpolation-based filter, and Partition based HAAR wavelet transform based filter. This technique makes use of the multi-size window and trimming concepts. This method involves the Trimming concept and multi-size window concept.

Fig. 1 reveals the overall block diagram of the NRPMID filter. The 512x512 size dental grayscale I_N is fed as input and the final noise-free output is noted as $I_{NF.}$ The noise-added image is quoted as I_N. The assignment of $\propto = 5$ is made, and $\propto$ refers to the maximum permitted iterations. The minimum value of the noisy image is set in β^1. The maximum value of the noisy image is stored in β^2. In this work maximum of five iterations (itr) are used to resolve the noises. If itr=0 then Procedure_Iteration_0 is called. If itr=1 then Procedure_Iteration_1 is called, and so on. The window size γ is computed as $\gamma = itr + 1$. The noisy pixels which meet the condition $I_N^{i,j} \leq \beta^1 \;\; || \;\; I_N^{i,j} \geq \beta^2$, are stored in $I_{NI.}^{i,j} = 0$, otherwise stored as non-noisy pixels by assigning $I_{NI.}^{i,j} = 1$. Then, the particular iteration is called based on the value of itr-number. Finally the objective function checks for the next progress, by verifying any modification in the current and previous noise-free images.

A. Itr_0 Process

The three components Mean computation, Median computation, and Bi-linear interpolation are used in the design of the itr_0 process. A 3x3 size window is extracted from the noisy locations, and the non-noisy information/intensity is stored in the linear vector δ. This scenario is noted as the trimming process. The trimming process yields a maximum of eight elements for a 3x3 window. The non-noise element count is stored in TNC. If the TNC is in between one and four, then the mean-oriented denoising is progressed. Otherwise, the standard deviation of δ is computed, and if it is less than or equal to 3.2 then the median oriented denoising is progressed, otherwise Bi-linear interpolation [30] oriented denoising is progressed. The denoised outputs are assigned in $I_{NF}^{i,j}$. Suppose the TNC is equal to zero then the original intensity is stored in $I_{NF}^{i,j}$. This process is employed for the entire noisy pixels of the noisy image.

B. Itr_1 Process

The Itr_1 procedure is designed using a new set of rules and four computations viz. Mean, Median, Partition oriented median, and Bi-cubic interpolation. The Itr-0 output is fed as input and quoted as I_N. A 5x5 window size window is extracted from a noisy pixel, and the trimmed elements are stored in the linear array δ. Herein, the maximum numbers of non-noisy elements are 16. The term TNC is also computed. If TNC>0 & TNC<=4 then Mean oriented denoising is approached. If TNC>4 & TNC<=8 then Median oriented

denoising is approached. If TNC>8 & TNC<=12 then Partition oriented median-based denoising is approached, and it can be calculated by a range of equations from (1) to (4).

$$M_I = FindMedian(\delta) \quad (1)$$

$$M_{P1} = FindMedian(\delta^{0\ to\ \left(\frac{TNC}{2}\right)-1}) \quad (2)$$

$$M_{P2} = FindMedian(\delta^{\left(\frac{TNC}{2}\right)\ to\ TNC-1}) \quad (3)$$

$$M_P = \begin{cases} M_{P1}, if\ abs(M_{P1} - M_I) \leq abs(M_{P2} - M_I) \\ M_{P2}, otherwise \end{cases} \quad (4)$$

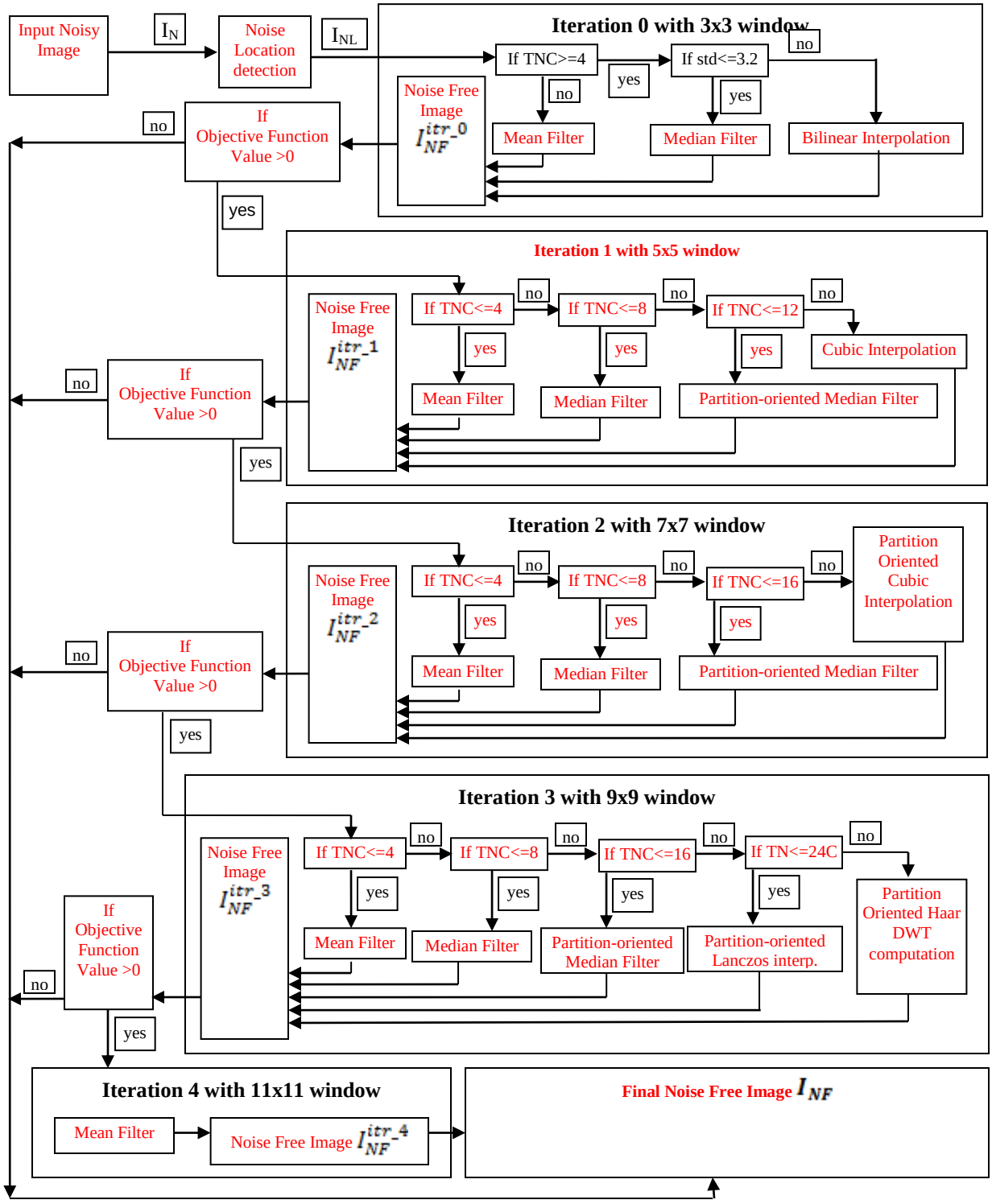

Fig. 1. Working of the Proposed NRPMID Filter.

Where

M_I - Integrated-median, M_{P1}- Partition_1 oriented median, M_{P2}- Partition_2 oriented median, and M_P - Final partition-oriented median.

The M_I is computed from the whole data of δ. Herein, δ is divided into a couple of divisions, and they are partition_left and partition_right. The Partition_left is used to compute M_{P1}, and partition_right is used to calculate M_{P2}.

The closest part of M_I is determined via Equation (4) to find the M_P. If TNC>12 & TNC<=16 then Bi-cubic interpolation-oriented noise removal is approached. The denoised outputs are assigned in $I_{NF}^{i,j}$. Suppose the TNC is equal to zero then the original intensity is stored in $I_{NF}^{i,j}$. The noisy pixels in the entire noisy image are processed using this method.

C. Itr_2 Process

The Itr_2 procedure is incorporated by a 7×7 size neighbor window, new rules, and 4 computations such as Mean, Median, Partition oriented median, and Partition oriented Bi-cubic interpolation. Herein, a maximum of 24 non-noisy neighbors can be extracted. If$TNC > 0$ &$TNC <= 4$, then mean-oriented noise removal is progressed. If$TNC > 4$ & $TNC <= 8$, then median value is used for noise cancellation. If $TNC > 8$ & $TNC <= 16$ then Partition oriented median is the source for noise suppression. If $TNC > 16$ & $TNC <= 24$ then Partition oriented Bi-cubic based noise removal is progressed using the range of equations (5) to (8).

$$BC_I = FindBCubicValue(\delta) \quad (5)$$

$$BC_{P1} = FindBCubicValue(\delta^{0\ to\ (\frac{TNC}{2})-1}) \quad (6)$$

$$BC_{P2} = FindBCubicValue(\delta^{(\frac{TNC}{2})\ to\ TNC-1}) \quad (7)$$

$$BC_P = \begin{cases} BC_{P1}, & if\ abs(BC_{P1} - BC_I) \leq abs(BC_{P2} - BC_I) \\ BC_{P2}, & otherwise \end{cases} \quad (8)$$

where

BC_I - Integrated-BiCubic data

BC_{P1} - Partition_1 oriented Bi-cubic data.

BC_{P2} - Partition_2 oriented Bi-cubic data.

BC_P - Final partition oriented Bi-cubic data.

This process is repeated for the whole noisy pixels of the noisy image.

D. Itr_3 Process

The Itr_3 procedure is carried out via a 9×9 side window, and the five techniques like i) Mean ii) Median, iii) Partition oriented median, iv) Partition oriented Lanczos interpolation and v) Partition oriented Haar-Wavelet transform. Herein, a maximum of 32 non_noisy neighbours are collected. The noise reduction is performed based on Fig. 1 corresponding to iteration_3. If TNC>16 & TNC<=24 then Partition oriented Lanczos interpolation-based denoising is progressed. Haar_wavelet transform [32] which is a discrete wavelet transform, is utilized to characterize the image. If $TNC > 24$ & $TNC <= 32$ then Partition-oriented Haar_wavelet transform-based noise removal is progressed, and it can be done via the range of equations (9) to (12).

$$HW_I = FindHaarWTValue(\delta) \quad (9)$$

$$HW_{P1} = FindHaarWTValue(\delta^{0\ to\ (\frac{TNC}{2})-1}) \quad (10)$$

$$HW_{P2} = FindHaarWTValue(\delta^{(\frac{TNC}{2})\ to\ TNC-1}) \quad (11)$$

$$HW_P = \begin{cases} HW_{P1}, & if\ abs(HW_{P1} - HW_I) \leq abs(HW_{P2} - HW_I) \\ HW_{P2}, & otherwise \end{cases} \quad (12)$$

where

HW_I - Integrated-HaarWT data.

HW_{P1} - Partition_1 oriented HaarWT data.

HW_{P2} - Partition_2 oriented HaarWT data.

HW_P- Final partition-oriented HaarWT data.

This process is continued for the whole noisy pixels of the noisy image.

E. Itr_4 Process

The Itr_4 procedure is designed based on 11×11 size window and the Mean computation. The δ and TNC are found. If $TNC > 0$ then mean of δ is assigned in the location of noisy data. If $TNC = 0$ then mean of the whole 11×11 size neighbors is assigned as the noise-free data in the corresponding noise location.

In this model, the proposed NRPMID filter reduces the salt and pepper noise or impulse noise in the X-ray dental images.

IV. Discussion and Analysis

The MATLAB 15 version was used to build this novel technique. The NMIC Dental X-Ray image dataset [26] and the VAHAB Dental X-Ray image dataset [25] are the databases that were used in this study. 150 dental teeth X-Ray images from each dataset are used in this study as test images. On dental X-ray images, the proposed NRPMID approach is compared to the following three denoising techniques.

- Image denoising using Newton Thiele filter (ID-NTHF)[27].
- Image noise removal based on adaptive fuzzy switching median filter (ID-FSMF) [28].
- Image denoising based on Adaptive Sequentially Weighted Median Filter (ID-AWMF) [29].

The denoising of the proposed technique for 98.32 percent noise corruption is shown in Fig. 2. The input image used in this instance was obtained from the VAHAB database. Fig.

2(a) points out the original image, Fig. 2(b) focuses on the noisy image, and Fig. 2(c) shows the final noise-free image.

1) Accuracy: Accuracy is metric used to evaluate how precisely the measured value or findings reflect the real or the original values. The Table I represents the accuracy analysis obtained by the proposed and the other denoising models.

From Fig. 3, it can be observed that the proposed NRPMID filter achieves the highest accuracy value of 0.96% when compared to other models, which indicates that it efficiently reduces the noises from the input image.

2) Mean Square Error (MSE): Mean Square Error is a metric used to measures the amount of error in statistical models. It assesses the average squared difference between the observed and predicted values. When a model has no error, the MSE equals zero. As model error increases, its value increases. The mean squared error is also known as the mean squared deviation (MSD).

In this analysis, the MSE of the proposed NRPMID filter and the other denoising models are analyzed. It is evident from the results demonstrated in Table II and Fig. 4 that the proposed NRPMID filter achieves the lowest MSE value of 0.037.

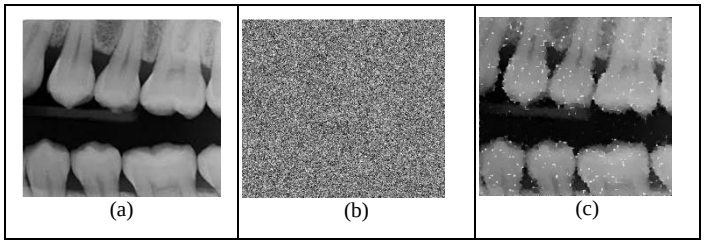

Fig. 2. Noise Removal NRPMID for 98.32% Noise Corruption, (a) Original Input Image (b) Noise Added Image (c) Noise Free Image.

TABLE I. ACCURACY ANALYSIS

Denoising method	Accuracy (%)	
	NMIC database	*VAHAB database*
ID-NTHF	0.74	0.76
ID-FSMF	0.77	0.79
ID-AWMF	0.89	0.90
NRPMID	0.95	0.96

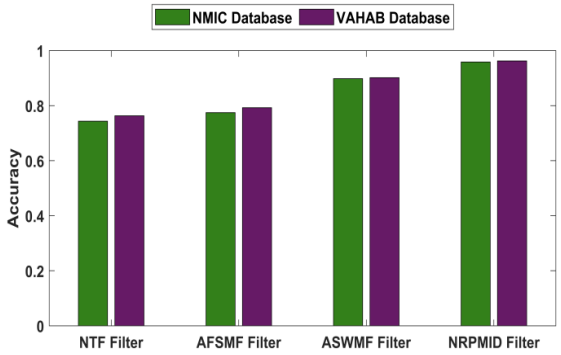

Fig. 3. Accuracy Analysis on Four Methods and Two Datasets.

TABLE II. MSE ANALYSIS

Denoising method	MSE	
	NMIC database	*VAHAB database*
ID-NTHF	0.256	0.236
ID-FSMF	0.225	0.207
ID-AWMF	0.101	0.098
NRPMID	0.041	0.037

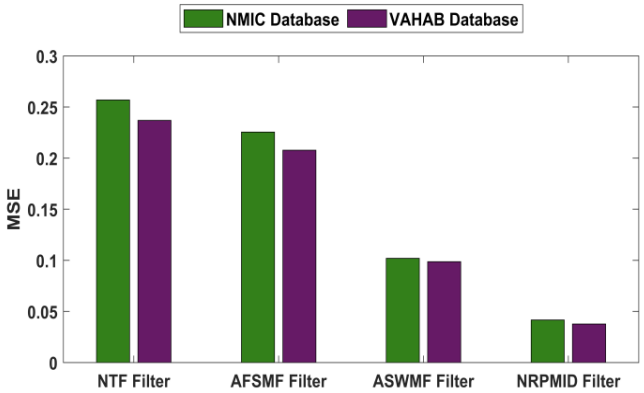

Fig. 4. MSE Analysis for Four Methods and Two Datasets.

3) Average MSE analysis: The average MSE analysis is also computed in this analysis and results are represented in Table III.

TABLE III. AVG. MSE ANALYSIS FOR 90% NOISE CORRUPTION

Denoising method	Avg. MSE	
	NMIC database	*VAHAB database*
ID-NTHF	656.276	629.623
ID-FSMF	591.679	533.435
ID-AWMF	427.640	391.810
NRPMID	131.555	124.198

The proposed NRPMID filter's effectiveness in the average MSE analysis case with noise corruption of 90% is shown in Table III. When compared to other approaches, the NRPMID method produces low MSE values.

4) PSNR Analysis: The Peak Signal to Noise Ratio (PSNR) analysis is computed and the High PSNR means better denoising.

The average PSNR values with noise corruption of 90% can be seen in Fig. 5. Each database's 150 images are used to compute it. It demonstrates that the NRPMID filter can be used to restore more successfully than the conventional filters.

5) Root Mean Square Error (RMSE): The mathematical derivation for computing RMSE is provided in Equations (13).

$$Error_{RMSE} = \sqrt{\frac{\sum_{i=1}^{N}(p_i - r_i)^2}{T}} \quad (13)$$

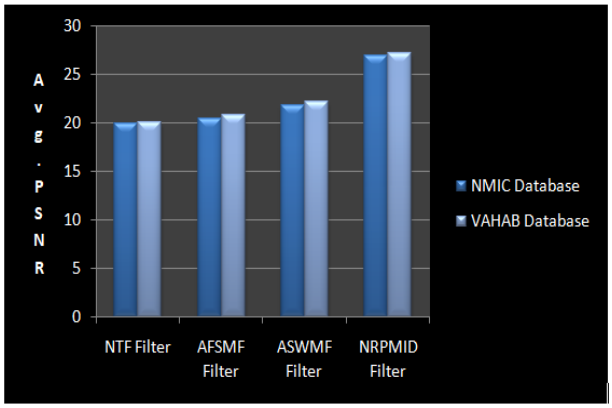

Fig. 5. Average PSNR Analysis for Noise Corruption of 90%.

TABLE IV. RMSE ANALYSIS

Denoising method	MSE	
	NMIC database	*VAHAB database*
ID-NTHF	0.506	0.486
ID-FSMF	0.474	0.455
ID-AWMF	0.319	0.314
NRPMID	0.203	0.194

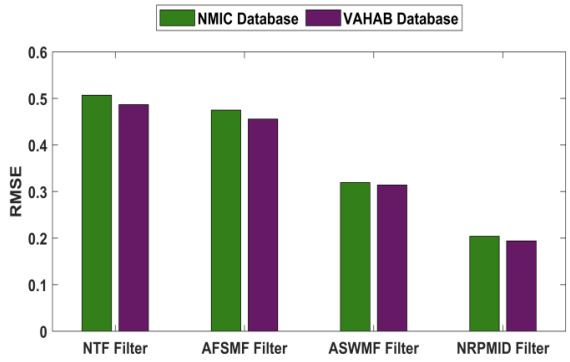

Fig. 6. RMSE Analysis.

The RMSE analysis of the proposed NRPMID filter and other denoising models are expressed in Table IV and Fig 6. From the results, it is evident that the proposed work achieves the lowest RMSE value of 0.194 which indicates the accuracy of the NRPMID filter is high.

6) Structural Similarity Index (SSIM): A perceptual metric called the Structural Similarity Index (SSIM) measures the loss of image quality put on by denoising [33]. The denoising Quality is better if the MSSIM value is high.

The average SSIM results in 60% noise corruption, as shown in Fig. 7. It illustrates that the proposed NRPMID approach obtains higher SSIM values than the traditional methods.

7) Average IEF analysis: The IEF analysis is used to assess the effectiveness of salt and pepper noise denoising in dental X-ray images. Better denoising quality is correlated with higher IEF and vice versa [34].

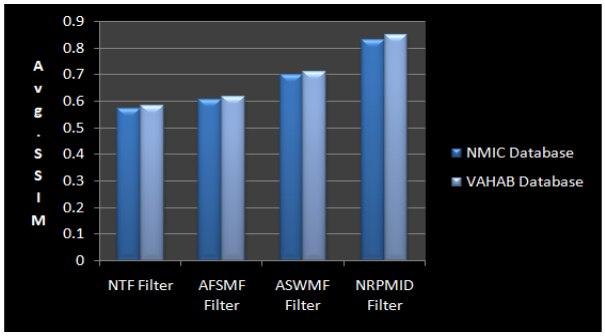

Fig. 7. Avg. SSIM Analysis for 60% Noise Corruption.

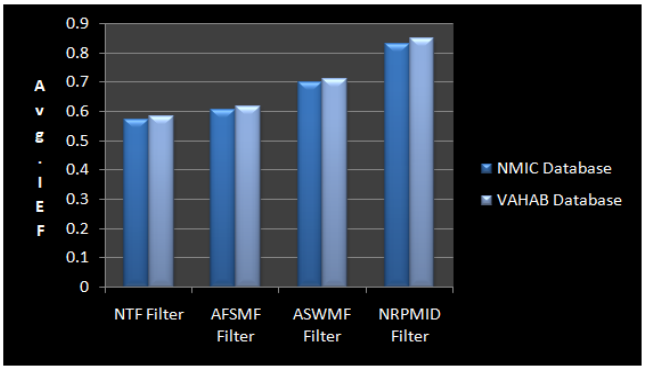

Fig. 8. Avg. IEF Analysis for 90% Noise Corruption.

The average IEF analysis values for noise corruption of 90% are shown in Fig. 8. The proposed NRPMID filter outperforms existing techniques in terms of high IEF values. The VAHAB database is the finest database to support the proposed work, according to the analysis.

V. CONCLUSION

This research proposes the NRPMID filter to reduce the impulse noise in teeth X-ray medical images. The NRPMID filter can resolve salt and pepper noise from the dental X-Ray images, which are even corrupted by 98.32%. The proposed filter improves the visual quality of dental X-ray images. It assists dental pathologists in having an accurate diagnosis. The time complexity of this approach is significantly less. The analysis section proves the noticeable results of the NRPMID filter than the existing denoising methods. The advantage of the method is simple and less costly. The drawback of the proposed system is the high computational time. In the future, this research can be extended to solve the Poisson noise in dental X-Ray images. Also, image enhancement techniques will be used to enhance the image quality.

REFERENCES

[1] Sumitra, P. "A comparative study algorithm for noisy image restoration in the field of medical imaging." International Journal of Advanced Information Technology (IJAIT) 6.1 (2016): 35-42.

[2] Kadam, Chaitali, and P. S. B. Borse. "A Comparative Study of Image Denoising Techniques for Medical Images." image 4.06 (2017).

[3] K. Shanida, R. Shayini, and C.S. Sindhu, "Dental image enhancement using wavelet decomposition and reconstruction", International Journal of Recent Advances in Engineering & Technology (IJRAET), vol. 4, issue 7, 2016.

[4] HosseinKhani, Zohreh, et al. "Adaptive real-time removal of impulse noise in medical images." Journal of medical systems 42.11 (2018): 1-9.

[5] Nitu Kumari, Kusum Kumari, Manisha Tigga and Sushanta Mahanty, "Noise detection and noise removal techniques in medical images", International journal of computer engineering and applications, vol. 10, special issue, 2016.

[6] K. Shanida, R. Shayini and C.S. Sindhu, "Dental image enhancement using wavelet decomposition and reconstruction", International Journal of Recent Advances in Engineering & Technology (IJRAET), vol. 4, issue 7, 2016.

[7] HosseinKhani, Zohreh, et al. "Adaptive real-time removal of impulse noise in medical images." Journal of medical systems 42.11 (2018): 1-9.

[8] Nitu Kumari, Kusum Kumari, Manisha Tigga and Sushanta Mahanty, "Noise detection and noise removal techniques in medical images", International journal of computer engineering and applications, vol. 10, special issue, 2016.

[9] Khan, Sajid, and Dong-Ho Lee. "An adaptive dynamically weighted median filter for impulse noise removal." EURASIP Journal on Advances in Signal Processing 2017, no. 1 (2017): 1-14.

[10] Kandemir, Cengiz, Cem Kalyoncu, and Önsen Toygar. "A weighted mean filter with spatial-bias elimination for impulse noise removal." Digital Signal Processing 46 (2015): 164-174.

[11] Thanh, Dang Ngoc Hoang, and Serdar Engínoğlu. "An iterative mean filter for image denoising." IEEE Access 7 (2019): 167847-167859.

[12] P. Gouchol, L. Jyh-charn and N.A. Sanju, "Selective removal of impulse noise based on homogeneity level information", IEEE Transactions on image processing, vol. 12, no. 1, pp. 85-92, 2003.

[13] Chen PY, Lien CY. An efficient edge-preserving algorithm for removal of salt-and-pepper noise. IEEE Signal Process Lett. 2008;15(2):833–6.

[14] K.S. Srinivasan and D. Ebenezer, "A new fast and efficient decision-based algorithm for removal of High-Density impulse noises", IEEE Signal processing letters, vol. 14, no. 3, pp. 189-192, 2007.

[15] K.K.V. Toh and N.A.M. Isa, "Noise Adaptive Fuzzy Switching Median Filter for Salt and Pepper noise reduction", IEEE Signal Processing letters, vol. 17, no. 3, pp. 281-284, 2010.

[16] H. Shi, J. Shao, D. Du, B. Chang and H. Cao, "Noise Reduction of the Real-time X-ray Image Based on Modified Adaptive Local Noise Reduction Filter", IEEE, 4th International Congress on Image and Signal Processing, 2011.

[17] B.H. Tracey, E.L. Miller, M. Schiefele, C. Alvino and O.A. Kofahi, "Denoising approaches for X-ray personnel screening systems", IEEE Conference on Technologies for Homeland Security (HST), 2012.

[18] Kundu R, "Structural Enhancement of Digital X-ray Image of Bone with a Suitable Denoising Technique", Indian conference on medical informatics and telemedicine (ICMIT), 2013.

[19] K.Shanida, R. Shayini and C.S. Sindhu, "Dental Image Enhancement Using Wavelet Decomposition and Reconstruction". International Journal of Recent Advances in Engineering & Technology (IJRAET), vol. 4, issue 7, pp. 2347 -2812, 2016.

[20] S.U. Khan, M. Ishaq, N. Ullah, A. Ahamd and I. Ahmed, "A novel algorithm for removal of noise from X-Ray images", International Journal of Computer Science and Information Security, vol. 14, issue 10, 103-109, 2016.

[21] H. Markarian, and S. Ghofrani, "High–TV based CS framework using MAP estimator for SAR image enhancement", IEEE journal of selected topics in applied earth observations and remote sensing, vol. 10, issue 9, pp. 4059–4073, 2017.

[22] Zhang P, Li F. A new adaptive weighted mean filter for removing salt-and-pepper noise. IEEE Signal Process Lett. 2014; 21(10):1280–3.

[23] G. Naouel, M.C. Olfa, M. Mokhtar and M. Jerome, "Evaluation of DWT denoise method on X-ray images acquired using flat detector", IEEE 4th Middle East Conference on Biomedical Engineering (MECBME), 2018.

[24] I. Mandic, H. Peic, J. Lerga and I. Stajduhar, "Denoising of X-ray images using the Adaptive Algorithm Based on the LPA-RICI Algorithm", Journal of imaging, vol. 4, issue 34, pp. 1-15, 2018.

[25] Vahab database: Accessed from < https:// mynote book.labarchives.com/share/Vahab/MjAuOHw4NTc 2Mi8xNi9 UcmVlTm9kZS83NzM5OTk2MDZ8NTIuOA>, Accessed on [25-Mar-2021].

[26] NMIC database: Accessed from: <https://data.mendeley.com/ datasets/hxt48yk462/1>, Accessed on [25-Mar-2021].

[27] Tian Bai and Jieqing Tan, "Automatic detection and removal of high-density impulse noises", IET image processing, vol. 9, Issue 2, pp. 162 - 172, 2015.

[28] Ayyaz Hussain and Muhammad Habib, "A new cluster-based adaptive fuzzy switching median filter for impulse noise removal", SPRINGER, Multimedia Tools and applications, vol. 76, pp. 22001–22018, 2017.

[29] Jiayi Chen, Yinwei Zhanz and Huying Cao," Adaptive Sequentially Weighted Median Filter for Image Highly Corrupted by Impulse Noise", IEEE Access, vol. 7, pp. 158545 - 158556, 2019.

[30] Bi-linear interpolation, Accessed from <https://theailearner.com/ 2018/ 12/29/image-processing-bilinear-interpolation/>, Accessed on [4-Apr-2021].

[31] Bi-cubic interpolation, Accessed from <https://medium.com/hd-pro/bicubic-interpolation-techniques-for-digital-imaging-7c6d86dc35dc>, Accessed on [4-Apr-2021].

[32] Haar Transform, Accessed from <https://en.wikipedia.org/wiki/ Haar_wavelet>, Accessed on [6-Apr-2021].

[33] SSIM, Accessed from <https://www.imatest.com/docs/ssim/>, Accessed on [5-Apr-2021].

[34] V. Jayaraj and D. Ebenezer, "A New Switching-Based Median Filtering Scheme and Algorithm for Removal of High-Density Salt and Pepper Noise in Images", EURASIP Journal on Advances in Signal Processing, Vol. 2010, pp. 1-11. 2010.